CHEMISTRY
A European Journal

A Journal of
ChemPubSoc Europe

Accepted Article

Title: Self-Assembled Multivalent (SAMul) Polyanion Binding - Impact of Hydrophobic Modifications in the Micellar Core on DNA and Heparin Binding at the Peripheral Cationic Ligands

Authors: Buthaina Albanyan, Erik Laurini, Paola Posocco, Sabrina Pricl, and David K. Smith

To be cited as: *Chem. Eur. J.* 10.1002/chem.201700177

Link to VoR: http://dx.doi.org/10.1002/chem.201700177

Supported by
ACES

WILEY-VCH

10.1002/chem.201700177

WILEY-VCH

FULL PAPER

Self-Assembled Multivalent (SAMul) Polyanion Binding – Impact of Hydrophobic Modifications in the Micellar Core on DNA and Heparin Binding at the Peripheral Cationic Ligands

Buthaina Albanyan,[a] Erik Laurini,[b] Paola Posocco,[b] Sabrina Pricl,[b] and David K Smith[a],*

Abstract: This paper reports a small family of cationic surfactants designed to bind polyanions such as DNA and heparin. Each molecule has the same hydrophilic cationic ligand, and a hydrophobic aliphatic group with eighteen carbon atoms with either one, two or three alkene groups within the hydrophobic chain (C18-1, C18-2 and C18-3). Dynamic light scattering indicates that more alkenes lead to geometric distortion, giving rise to larger self-assembled multivalent (SAMul) nanostructures. Mallard Blue and Ethidium Bromide dye displacement assays demonstrate that heparin and DNA have markedly different binding preferences, with heparin binding most effectively to C18-1, and DNA to C18-3, even though the molecular structural differences of these SAMul systems are buried in the hydrophobic core. Multiscale modelling suggests that adaptive heparin maximises enthalpically-favourable interactions with C18-1, while shape-persistent DNA forms a similar number of interactions with each ligand display, but with slightly less entropic cost for binding to C18-3 – fundamental thermodynamic differences in SAMul binding of heparin or DNA. This study therefore provides unique insight into electrostatic molecular recognition between highly charged nanoscale surfaces in biologically-relevant systems.

Introduction

Biological polyanions are involved in a wide range of medically important processes – for example, nucleic acids have great potential in gene therapy,[1] while glycosaminoglycans like heparin control coagulation processes.[2] The ability of synthetic systems to interact with polyanions is therefore of considerable interest, with much focus on the ability of cationic systems to bind polyanionic targets.[3] In the field of gene delivery, a key strategy has been to use cationic lipids, which self-assemble into nanoscale systems in order to bind DNA/siRNA.[4] Much research has focussed on the development of structure-activity relationships.[5] A number of reports have focussed on understanding the impact of hydrophobic modification on gene delivery.[6] It is known, for example, that alkene groups in the hydrophobic unit change the fluidity of the hydrophobic domain and modifying phase transition temperatures.[7]

We have described systems in which self-assembly is used to display specific ligands (rather than point charges) on nanostructure surfaces as exhibiting self-assembled multivalent (SAMul) binding.[8] There are inherent advantages of this approach such as ease of synthesis, ligand tunability, morphological programmability, and the ability to disassemble the nanostructures on demand. As such, we believe this SAMul approach offers some significant advantages over covalent polymeric or dendritic approaches commonly used to generate multivalent ligand arrays.[9] The use of SAMul arrays to achieve effective polyanion binding has been a particular recent interest, and in addition to DNA binding and gene delivery,[4-6,10] significant attention has also focussed on using this approach to bind glycosaminoglycans, such as heparin.[11] Of course, in general terms, any cationic species will bind to an anionic one, and as is often noted, charge density will play a dominant role in determining the affinity of interaction.[12] However, we have recently focussed on exploring whether different polyanions, such as heparin or DNA, exhibit different binding preferences towards different SAMul systems, demonstrating that factors such as choice of ligand[13] and chirality[14] can significantly impact on the binding preference, irrespective of charge density. The ligands are located at the nanoscale binding interface and play the key role in mediating the interactions between the SAMul cation and the polyanion – there is a clear molecular-scale mechanism for this effect. Multiscale modelling methods in which atomistic and mesoscale methods are combined, provide a uniquely powerful toolkit,[15] and have allowed us to gain fundamental insight into such molecular recognition processes at nanoscale binding interfaces.[10,11b,c,13,14b]

In this paper, we explore the effect of changing the hydrophobic unit on selectivity. Although the effect of hydrophobe is relatively well understood in the field of gene delivery,[6] it has not previously been considered in terms of fundamental impacts on polyanion binding selectivity. Although these units are responsible for driving self-assembly, once this process is complete, they are buried inside the SAMul nanostructure and might not be expected to directly impact on binding. We therefore designed a family of compounds with identical ligands appended to a hydrophobic unit, which, in each case, had the same number of carbon atoms – only the degree of unsaturation differed (Fig.

[a] Prof. D. K. Smith and Dr B. Albanyan
Department of Chemistry
University of York
Heslington, York, YO10 5DD, UK
Fax: (+44) 1904 324516
E-mail: david.smith@york.ac.uk
[b] Prof. S. Pricl, Dr E. Laurini, Dr. P. Posocco
Simulation Engineering (MOSE) Laboratory, Department of Engineering and Architecture (DEA),
University of Trieste
34127, Trieste, Italy
E-mail: sabrina.pricl@di3.units.it

Supporting information for this article is given via a link at the end of the document

10.1002/chem.201700177

1). We then investigated the ability of these structures to bind DNA and heparin, reasoning this would help provide a structure-activity relationship, relevant in developing SAMul systems for potential applications in fields such as gene delivery or coagulation control.

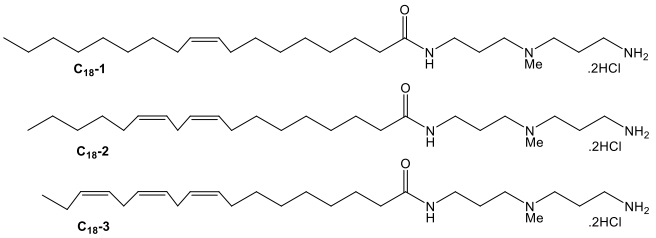

Figure 1. Compounds investigated in this paper, C18-1, C18-2 and C18-3, with one, two and three *cis*-alkene groups respectively.

Results and Discussion

For the purposes of this structure-activity study, amphiphilic molecules with the same di-(aminopropyl)-methylamine ligand were synthesised (Fig. 1) each of which could, in principle, self-assemble into micelles displaying a cationic ligand surface. As hydrophobe we selected naturally occurring *cis*-fatty acids – oleic (1 alkene), linoleic (2 alkenes) and linolenic (3 alkenes) acids. These molecules were synthesised using TBTU-mediated peptide coupling with an appropriate Boc-protecting group strategy (see ESI). The synthesis yielded C18-1, C18-2 and C18-3 in which the latter number refers to the number of alkene groups. Each of these compounds has an identical nominal +2 ligand charge at physiological pH.

We initially quantified self-assembly using a Nile Red assay[16] in 150 mM NaCl and found that on increasing concentration, all of the compounds formed micelles and led to an increase in Nile Red fluorescent emission. Analysis of the data enabled estimation of critical micelle concentrations (CMCs). These were found, in general terms, to increase as the degree of unsaturation increased. We propose that the presence of alkene groups disrupts lipid packing within the interior of the micellar nanostructure – indeed, such effects are well-known in surfactant chemistry with unsaturated lipids showing a significantly greater degree of fluidity as a result of the geometric disruption to the extended hydrophobic chain induced by the insertion of the rigid alkene group with its precise geometric demands.[17] It should be noted that there is little difference in CMC between C18-2 and C18-3, which may suggest that once two alkenes have been introduced, the presence of a third has relatively little additional adverse effect.

We then used dynamic light scattering (DLS) to characterise the assemblies. Table 1 presents volume distribution data, which indicates an increase in micellar diameter on increasing the level of unsaturation. Looking in detail at the intensity distribution data (see ESI) indicated that there was also a contribution from ill-defined larger aggregates (>100 nm) for each of the amphiphiles – however, the contribution of this increases in the order C18-1<C18-2<C18-3, which would suggest less controlled self-assembly as the number of alkenes increases. This would suggest that the most effective aggregation into small micelles (<10 nm) is achieved by C18-1, while the introduction of more alkenes begins to hinder effective self-assembly and gives rise to a slightly greater degree of relatively uncontrolled aggregation. The ζ-potential values were all positive, as expected for these cationic self-assembling structures. The observed charge density was slightly greater for C18-2 and C18-3 than for C18-1, which suggested that more self-assembling units may be incorporated into the more unsaturated structures (consistent with their larger diameters).

Table 1. Experimental characterisation of self-assembled micelles performed in 150 mM NaCl, 10 mM PBS, pH 7.4) using Nile Red assay to give CMC and dynamic light scattering (150 mM NaCl, 10 mM Tris HCl, pH 7.4) to give diameter and ζ-potential.

Compound	CMC / μM	Diameter (nm)	ζ (mV)
C18-1	42 ± 3	5.2 ± 0.5	+64.1 ± 0.6
C18-2	82 ± 2	6.4 ± 0.4	+72.9 ± 3.7
C18-3	78 ± 10	7.6 ± 0.3	+72.9 ± 2.5

Combined atomistic and mesoscale molecular simulations confirmed the dominant self-assembly of all compounds into spherical micelles, as shown by the images reported in the first row of Table 2. The *in silico* predicted micellar diameters and ζ-potentials (Table 2) are in excellent agreement with the corresponding experimental data (Table 1). Importantly, the estimated values of the aggregation number N_{agg} increases on passing from C18-1 to C18-3 (i.e., 28, 32 and 35 for micelles formed by compounds C18-1, C18-2, and C18-3, respectively, Table 2), supporting the hypothesis above, i.e., increasing the degree of unsaturation results in greater incorporation of units into the corresponding self-assembled nanostructures.

Table 2. *In silico* characterisation of self-assembled micelles formed by compound C18-1, C18-2, and C18-3 in water at 150 mM NaCl.

	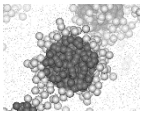 C18-1	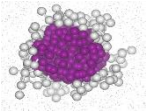 C18-2	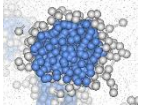 C18-3
Diameter (nm)	5.4 ± 0.4	6.2 ± 0.2	7.2 ± 0.2
N_{agg}	28 ± 2	32 ± 1	35 ± 1
ζ (mV)	+63.2	+73.4	+75.2

We then investigated the ability of these nanostructures to bind polyanions using two experimental dye displacement assays. In order to monitor heparin binding, we made use of the Mallard Blue (MalB) assay developed in our laboratory,[18] in which MalB is displaced from its complex with heparin. To monitor DNA binding ability, we employed the well-known Ethidium Bromide (EthBr) assay in which EthBr is displaced from its complex with DNA.[19] The data from these assays are presented in Table 3. The EC_{50} values reflect the concentration of self-assembled

10.1002/chem.201700177

multivalent binder required to displace 50% of the relevant dye, while the CE_{50} values reflect the charge excess (cationic binder:polyanionic target) at which 50% displacement of dye takes place. Low values indicate stronger binding, as they mean less compound is required to displace the competitor dye from the polyanionic target. It is important to note that the CE_{50} and EC_{50} values for the two different assays cannot be directly compared with one another, as they take place at different concentrations of polyanion, different concentrations of indicator dye, and the relative strengths of the MalB:heparin and EthBr:DNA complexes are also different. However, this approach is ideal for comparing the relative ability of this family of SAMul binders to interact with each of the polyanions under the conditions of the same binding assay, and trends within each set of data, induced by the introduction of unsaturation into the hydrophobic core of the SAMul nanostructure, can be meaningfully elucidated.

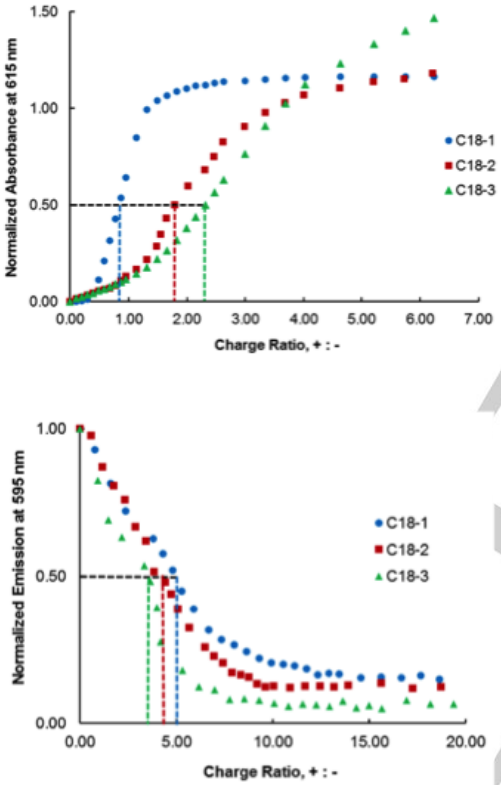

Figure 2. (Top) Heparin binding curves from MalB-displacement assay experiments (25 μM MalB and 27 μM heparin (based on a typical tetraanionic disaccharide repeat unit) in 150 mM NaCl, 10 mM Tris HCl, pH 7.4. (Bottom) DNA binding curves from EthBr-displacement assay experiments (5.07 μM EthBr and 4.0 μM DNA (based on a typical singly-charged nucleotide) in 150 mM NaCl, 10 mM HEPES, pH 7.4.

The heparin binding ability decreases as the level of unsaturation increases, with the CE_{50} increasing from 0.8 to 1.8 to 2.3 for C18-1, C18-2 and C18-3 respectively. (Table 2, Fig. 2 (top)). These changes in binding are significant and well beyond the range of error, suggesting that the modification to the hydrophobic unit has significant impact on SAMul binding to heparin. In order to probe these differences in binding in more detail, we employed multiscale modelling methods (see below). For DNA binding, however, a different trend was observed with the CE_{50} values of 5.0, 4.3 and 3.5 for C18-1, C18-2 and C18-3 respectively (Table 2, Fig. 2 (bottom)) indicating a slight strengthening of binding. It should be noted that considering the error ranges, the differences in DNA binding are relatively small compared to those for heparin binding – however, DNA nonetheless has a preference for C18-3.

We note that for C18-1 the EC_{50} value for heparin binding are close to the CMC values. This may suggest that self-assembly of an unbound micelle is a pre-requisite for heparin binding. However, for C18-3 (and to some extent C18-2) the EC_{50} values are below the CMC values – which may suggest that the self-assembly of the relatively poorly assembling C18-3 (and C18-2) is being assisted by the heparin binding event. Furthermore, the EC_{50} values for DNA binding are all well below the CMC values. Indeed, it is well-known that polyanions can induce self-assembly of cationic micelles, lowering the apparent CMC, and we propose this can occur with binding acting to reinforce self-assembly (and *vice versa*).[20]

Table 3. Heparin and DNA Binding Parameters: CE_{50} (cation:anion charge excess at which 50% of indicator dye is displaced from its complex) and EC_{50} (effective concentration at which 50% of dye is displaced, μM). Heparin binding performed with 25 μM MalB and 27 μM heparin (based on a typical tetraanionic disaccharide repeat unit) in 150 mM NaCl, 10 mM Tris HCl, pH 7.4. DNA binding performed on 5.07 μM EthBr and 4.0 μM DNA (based on a typical singly-charged nucleotide) in 150 mM NaCl, 10 mM HEPES, pH 7.4.

		C18-1	C18-2	C18-3
CE_{50}	Heparin	0.80 ± 0.05	1.8 ± 0.1	2.3 ± 0.2
	DNA	5.0 ± 0.7	4.3 ± 0.5	3.5 ± 0.4
EC_{50} / μM	Heparin	43 ± 3	97 ± 7	124 ± 10
	DNA	10.0 ± 0.4	8.6 ± 1.0	7.0 ± 0.8

There were some problems with the heparin binding assay, particularly with C18-3 where hierarchical aggregation (see below) giving rise to a degree of light scattering and increasing the absorbance more than expected (Fig. 2 (top)). It is important to note that this mainly affected the latter stages of the titration when excess binder was present – by which point the CE_{50} value had already been achieved. Furthermore, in the event of a small amount of light scattering from hierarchical aggregation being present at the CE_{50} value, this would actually act to raise the CE_{50} value of C18-3 – reinforcing the trend reported here in which this system is the weakest heparin binder. We are therefore confident that the CE_{50} values are valid, and that the reported trends in heparin binding reported in this manuscript are robust.

Interestingly, we have previously reported the synthesis of the fully saturated member of this family of amphiphiles, which can be considered C18-0 in the nomenclature used here (previously named C18-DAPMA).[21] This fully saturated compound experienced some solubility problems and analysis of DLS by volume distribution indicated the formation of larger assemblies (93±26 nm).[21] In terms of heparin binding, the CE_{50}

10.1002/chem.201700177

was found to be 0.68 ± 0.09 and the EC_{50} was 37 ± 5 mM.[21] The heparin binding performance of C18-0 is therefore equivalent to, or better than, that of C18-1, continuing the trend in which those systems with fewer alkenes are more effective heparin binders. However, given the differences in native self-assembled morphology between C18-0 and the other amphiphiles studied here, we decided not to extend the study of this system further.

Atomistic molecular dynamics (MD) simulations[22] were then performed in an attempt to reproduce and understand these differences in binding selectivities. Figure 3 shows equilibrated MD snapshots of the complexes formed between the self-assembled micelles of compounds C18-1, C18-2, and C18-3 and heparin (top) and DNA (bottom), respectively. A cursory glance at these images already reveals that, in passing from units bearing a single unsaturation to those characterized by three double bonds in their hydrophobic tails (from left to right in the image), the number of SAMul ligands in the self-assembled structures which are in contact with heparin decreases (Fig. 3, top) whilst, in case of DNA, this number is nearly independent of this chemical factor (Fig. 3, bottom).

Quantitative analysis of the MD trajectories of each SAMul micelle/polyanion complex confirmed this qualitative perspective. Specifically, once self-assembled, C18-1 is able to exploit 19 out of the 28 units in effectively and permanently binding heparin (i.e., N_{eff} = 19), whereas a progressive decrease in N_{eff} is estimated when considering C18-2 and C18-3, which engage only 15/32 and 13/35 residues in contacting the polyanion, respectively. On the contrary, when bound to DNA, the calculated N_{eff} values are 16, 17 and 18 for the micelles formed by C18-1, C18-2, and C18-3 respectively. This structural difference is directly reflected in the corresponding per-residue effective free energy of binding values ΔG^* (Figure 4), as discussed below.

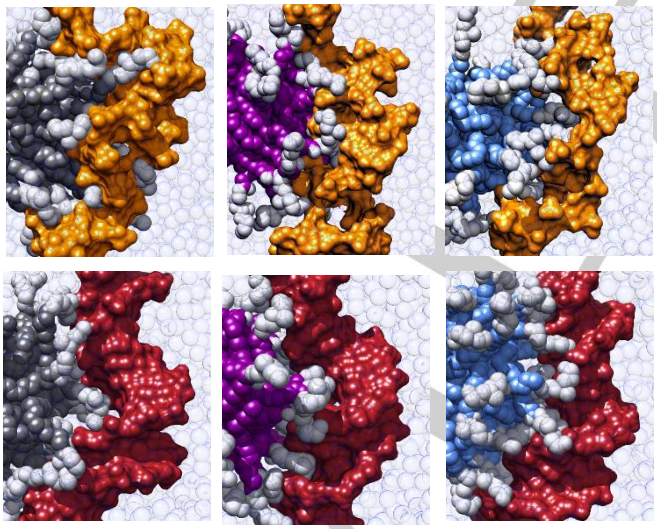

Figure 3. Equilibrated atomistic molecular dynamics (MD) simulation snapshots of (top) heparin and (bottom) DNA in complex with micelles formed by (from left to right) C18-1, C18-2, and C18-3. In all panels, micelles are shown as bi-colour spheres (hydrocarbon tails: C18-1, dark grey; C18-2, dark magenta, and C18-3, cornflower blue; polar heads: light grey). Heparin and DNA are portrayed via their van der Waals surfaces (coloured orange and firebrick, respectively). Water, ions and counterions are depicted as transparent spheres.

When considered from the perspective of a single effective SAMul ligand (Fig. 4A), in the case of heparin binding the more flexible 19 effective C18-1 units can maximize favourable enthalpic micelle/polyanion interactions (ΔH^* = -24.02 kJ mol^{-1}), thereby more than compensating for entropic penalty paid upon binding ($T\Delta S^*$ = -7.92 kJ mol^{-1}). Accordingly, the corresponding free energy is largely favourable (ΔG^* = -16.10 kJ mol^{-1}). However, on increasing the rigidity of the SAMul hydrocarbon chain as a consequence of the higher order of unsaturation, both the number and the efficacy of each effective unit available for heparin binding decreases. Thus, for C18-2 (N_{eff} = 15) ΔH^* = -17.76 kJ mol^{-1}, $T\Delta S^*$ = -5.55 kJ mol^{-1}, and ΔG^* = -12.21 kJ mol^{-1} while for C18-3 (N_{eff} = 13) the same thermodynamic quantities amount to -14.98 kJ mol^{-1}, -4.63 kJ mol^{-1}, and -10.35 kJ mol^{-1} respectively. It is interesting to observe that the inclusion of two or three carbon double bonds in the hydrophobic portion of the SAMul has a relative beneficial effect on the entropic term: as they become intrinsically more rigid, these molecules suffer progressively less entropic penalty than C18-1 on binding. However, these ligands are less able to reorganise, and the enthalpic component (ΔH^*) which accounts for the stabilising electrostatic intermolecular interactions between micelles and heparin decreases by about 10 kJ mol^{-1} on passing from C18-1 to C18-3. The net result of binding is enthalpically dominated, and the simulated ΔG^* values follow the same trend as the experimental CE_{50} values, i.e., C18-1 > C18-2 > C18-3.

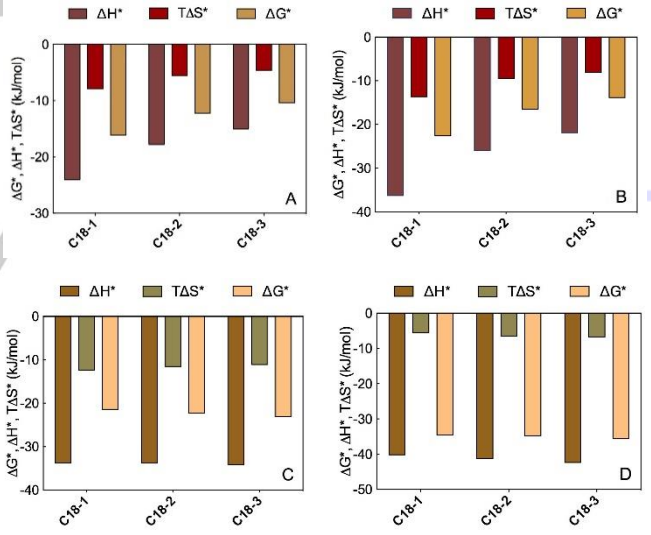

Figure 4. Per-residue effective free energy of binding (ΔG^*), and enthalpic (ΔH^*) and entropic ($T\Delta S^*$) components for: (A) micelles of C18-1, C18-2, and C18-3 complexed with heparin; (B) heparin sugars complexed with each of the SAMul micelles; (C) complexed with each of the SAMul micelles; (C) micelles of C18-1, C18-2, and C18-3 complexed with DNA; and (D) DNA bases complexed with each of the SAMul micelles.

On the other hand, for DNA binding, and again from the viewpoint of a single effective SAMul ligand (Fig. 4C) the enthalpic gain when self-assembled C18-1, C18-2, and C18-3 reorganise to maximise interactions with the nucleic acid is nearly constant, being equal to ΔH^* = -33.77 kJ mol^{-1}, -33.81 kJ mol^{-1}, and -34.15

10.1002/chem.201700177

kJ mol^{-1}, respectively. There is therefore only 0.38 kJmol^{-1} enthalpic difference between C18-1 and C18-3, in contrast to 9.04 kJmol^{-1} for heparin binding. The change in entropic component TΔS*, is also somewhat limited to ca. 1.3 kJ mol^{-1} on going from C18-1 to C18-3, in lieu of 3.3 kJ mol^{-1} observed on binding the same self-assembled micelles with heparin. As a result, the per-residue effective free energy of binding ΔG* of the different SAMul micelles in complex with DNA is less sensitive to molecular structure, that is ΔG* = -21.43 kJ mol^{-1}, -22.27 kJ mol^{-1}, and -23.07 kJ mol^{-1} for C18-1, C18-2, and C18-3, respectively, with the small increase reflecting a slkightly larger number of binding interactions. Compound C18-3 is therefore the slightly more effective DNA binder – in agreement with the experimental results. It should be noted that all of the absolute ΔG* values for DNA binding are significantly more favourable than those for heparin binding – consistent with the fact that effective DNA binding was experimentally observed at lower concentrations than heparin binding.

Applying the same analysis from the viewpoint of the polyanion, in the case of heparin (Fig. 4B) the variations of ΔG*, ΔH* and TΔS* with the number of alkenes parallel those experienced by the effective SAMul residues (Fig. 4A). Thus, heparin can compensate the higher entropic cost of binding C18-1 with a greater much enthalpic gain of its own, while progressively adapting the enthalpy/entropy ratio on increasing micellar rigidity (i.e., C18-2 and C18-3) via polyanion structural adaptation. Such a phenomenon was previously observed and reported by us for heparin binding to another set of SAMul molecules featuring the same chain but different polar heads,[13] evidence that helped us define heparin as a relatively flexible *adaptive* polyanion.[13,23] This property allows heparin to optimise binding to C18-1 on enthalpic grounds. From the perspective of DNA, ΔG* and its components are largely independent of the hydrophobic component of the SAMul units (Fig. 4D), confirming that each anion binds a cation with similar strength - reflecting the relatively rigid and *shape-persistent* nature of DNA.[13.23]

In combination, these observations support the conclusion that for heparin binding, a more flexible hydrophobic SAMul unit allows for an effective balance between favourable (i.e., enthalpic) and unfavourable (i.e., entropic) contribution to micelle/polyanion interactions, with enthalpy dominating the binding event. Increasing the structural rigidity of the SAMul unit results in overall worsening of heparin binding on enthalpic grounds. On the other hand, amphiphile tail rigidity has less influence on the ability of these SAMul micelles to organize for optimal shape-persistent DNA binding; hence, for all units the *in silico* estimated per-residue effective free energy of binding ΔG*, in agreement with the experimental EC_{50} values, are similar with C18-3 being slightly more effective than C18-2 which is in turn slightly better than C18-1.

We previously applied a similar thermodynamic analysis to the binding of self-assembled micelles with different surface ligands to heparin and DNA, and supported the simulations with experimental data from isothermal calorimetry.[13] In that case, it was demonstrated that the optimum heparin binder maximised its enthalpic term as a consequence of its ability to adapt and reorganise its binding sites to maximise interactions – a process which was reinforced by the relatively flexible and adaptive nature of polyanionic heparin.[13] This is directly equivalent to what is being observed here. For DNA binding, in our previous study,[13] each anionic site on the inflexible shape-persistent DNA formed equivalent interactions irrespective of the ligand, with binding preferences simply being driven by the number of interactions which could possibly form at the rigid binding interface (which in that case were quite significantly different in number). A similar but smaller effect is being observed here, with the small differences in binding originating from slightly different numbers of interactions at the rigid binding interface.

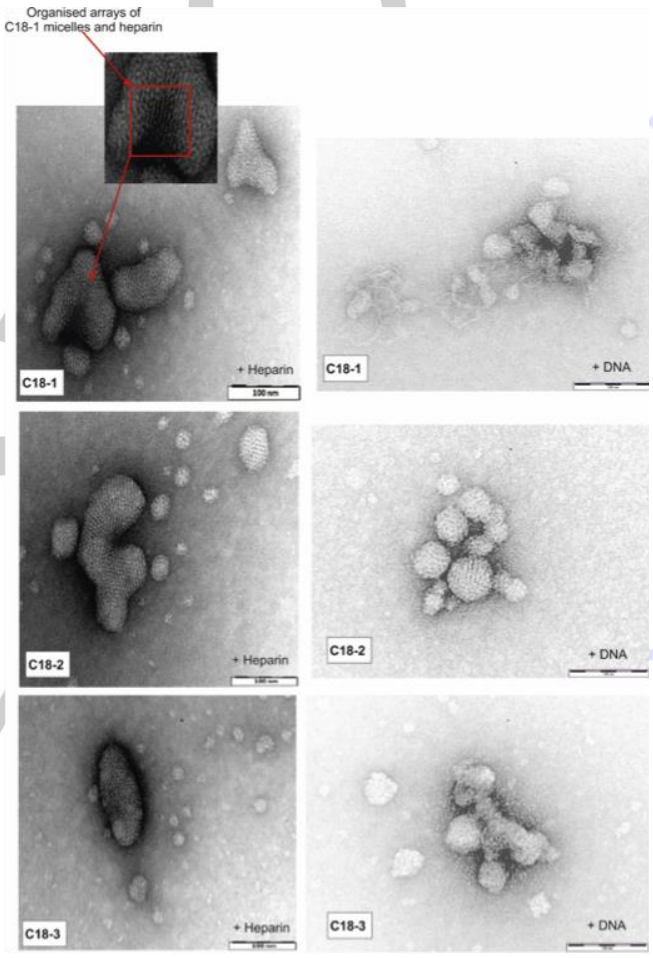

Fig. 5. TEM images of (top to bottom) C18-1, C18-2 and C18-3 bound to (left) heparin and (right) DNA – samples dried from solution onto the TEM grid. In each case, scale bar = 100 nm.

We then used transmission electron microscopy (TEM) to check that our self-assembled nanostructures remained intact on binding polyanions. For heparin binding, self-assembled micelles were clearly observed (Fig. 5, left), with sizes in general agreement with those observed by DLS for solution-phase self-assembly. In the presence of heparin, these micelles are hierarchically organised into a pseudo-crystalline nanoscale arrangement – we have recently fully characterised this process using a combination of SAXS, multiscale modelling and TEM for

a related system and determined that the spherical cationic SAMul nanostructures pack with the linear polyanions to form nanoscale two-dimensional ionic lattices on the TEM grid.[21] We can therefore confirm that the SAMul systems remains intact on binding polyanion targets, and that the presence of a highly charged electrostatic binding interface does not significantly disrupt these SAMul nanostructures. TEM also indicated similar hierarchical packing for DNA binding (Fig. 5, right) although the aggregates were somewhat less stable when exposed to the TEM electron beam.

To probe binding in more detail, we experimentally studied a 50:50 mixture of C18-1 and C18-3 to determine the effect on performance in these assays. In the heparin binding assay, a CE_{50} of 2.0 ± 0.3 was observed and in the DNA binding assay, the CE_{50} was 3.2 ± 0.2. The performance of the mixture was therefore much more closely similar to that of C18-3 rather than C18-1 (see Table 3). This suggests that the effect of alkene groups on the assembly and binding process dominates the performance of the mixed system in these binding assays as predicted and rationalised by multiscale modelling. This supports our hypothesis that the incorporation of alkenes into the hydrophobic unit, although not located at the nanoscale binding interface can directly influence the performance of the compounds in these DNA and heparin binding assays.

Given the clinical interest of heparin binding systems,[2] we also probed the ability of these compounds to bind heparin in more competitive conditions, performing the MalB assay in human serum (Table 4). As expected from our previous work on SAMul nanostructures,[11c] serum had an adverse effect on binding, and the CE_{50} values increased. As in buffer, C18-1 remained the most effective heparin binder, however, differences between all three systems somewhat decreased. This suggests serum has a generally adverse effect on self-assembly of the multivalent array and in particular disturbs the enthalpic benefits C18-1 employs for effective heparin binding. However, all three systems do still bind heparin to some extent, even in highly competitive human serum.

Table 4. Heparin Binding Parameters in Human Serum: CE_{50} (cation:anion charge excess at which 50% of indicator dye is displaced from its complex) and EC_{50} (effective concentration at which 50% of dye is displaced). Heparin binding performed with 25 μM MalB and 27 μM heparin (based on a typical tetraanionic disaccharide repeat unit) in 10 mM Tris HCl, pH 7.4

		C18-1	C18-2	C18-3
CE_{50}	Heparin	2.5 ± 0.2	3.4 ± 0.1	3.1 ± 0.1
EC_{50} / μM	Heparin	133 ± 10	182 ± 15	166 ± 2

Conclusions

In summary (Fig. 6), this is a rare report in which structure-activity effects are explored for binding self-assembling systems to two different polyanions. In the heparin binding assay, C18-1 > C18-2 > C18-3. Multiscale modelling allowed us to attribute this to the more effective nanoscale binding interface between C18-1 micelles and the adaptive polyanion heparin contributing a highly favourable enthalpic term to binding, in contrast to the less effective binding interface between the larger aggregates formed from rigid C18-3 and heparin. Conversely in our DNA binding assay, the differences between ligands are significantly smaller and C18-1 < C18-2 < C18-3. Multiscale modelling indicated that this shape-persistent polyanion formed similar binding interfaces with the SAMul nanostructures in each case, and there were only small differences in the apparent ΔG* caused primarily by the lower entropic costs of reorganisation of C18-3 compared with C18-1.

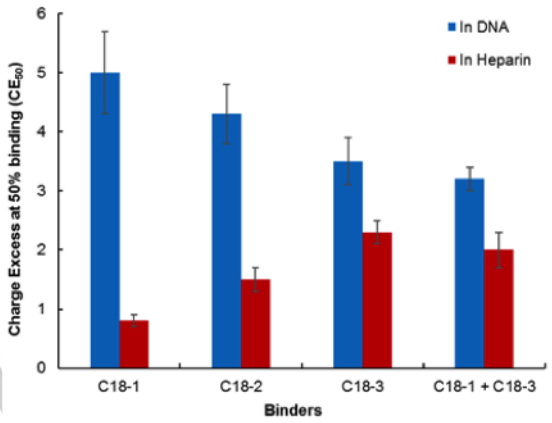

Figure 6. Summary of data for heparin and DNA binding extracted from MalB-displacement and EthBr-displacement assays respectively

We have therefore determined the surprisingly different binding preferences of different polyanions for SAMul systems. It is clear that even though the uncharged hydrophobic units are not directly involved at the binding interface, and are buried within the SAMul nanostructure, modifying them can have a profound effect on electrostatic binding at the periphery. This study therefore provides useful and unique insights into binding between highly charged nanoscale surfaces in biologically-relevant systems.

Acknowledgements

This work was supported by the Saudi Arabian Government via a PhD scholarship to BA.

Keywords: anion • electrostatics • molecular recognition • nanoscale • self-assembly

[1] R. Srinivas, S. Samanta, A. Chaudhuri, *Chem. Soc. Rev.*, **2009**, *38*, 3326-3338.

[2] S. M. Bromfield, E. Wilde, D. K. Smith, *Chem. Soc. Rev.*, **2013**, *42*, 9184-9185.

[3] K. Kogej, *Adv. Coll. Interface Sci.* **2010**, *158*, 68-83. (*b*) E. Kizilay, A. B. Kayitmazer, P. L. Dubin, *Adv. Coll. Interface Sci.*, **2011**, *167*, 24-37. (*c*) D. V, Pergushov, A. H. E. Muller, F. H. Schacher, *Chem. Soc. Rev.* **2012**, *41*, 6886-6901. (*d*) L. Piculell, *Langmuir*, **2013**, *29*, 10313-10329. (*e*) L. Chiappisi, I. Hoffmann, M. Gradzielski, *Soft Matter*, **2013**, *9*, 3896-3909.

(*f*) B. Lindman, F. Antunes, S. Aidarova, M. Miguel, T. Nylander, *Coll. J.*, **2014**, *76*, 585-594. (*g*) M. Siyawamwaya, Y. E. Choonara, D. Bijukumar, P. Kumar, L. C. Du Toit, V. A. Pillay, *Int. J. Polym. Mater. Polym. Biomater.*, **2015**, *64*, 955-968.

[4] (*a*) E. Junquera, E. Aicart, *Curr. Top. Med. Chem.*, **2014**, *14*, 663. (*b*) G. Navarro, J. Pan, V. P. Torchilin, *Mol. Pharm.*, **2015**, *12*, 301-313.

[5] (a) D. Niculescu-Duvaz, J. Heyes, C. J. Springer, *Curr. Med. Chem.*, **2003**, *10*, 1233-1261. (b) B. Martin, M. Sainlos, A. Aissaoui, N. Oudhiri, M. Hauchecorne, J.-P. Vigneron, J.-M. Lehn, P. Lehn, *Curr. Pharm. Des.*, **2005**, *11*, 375-394.

[6] For a review of the impact of the hydrophobic domain on gene delivery see: (*a*) D. F. Zhi, S. B. Zhang, B. Wang, Y. N. Zhao, B. L. Yang, S. J. Yu, *Bioconjugate Chem.*, **2010**, *21*, 563-577. For selected research papers in which the balance of hydrophobic and hydrophilic groups is tuned see: (*b*) D. Joester, M. Losson, R. Pugin, H. Heinzelmann, E. Walter, H. P. Merkle, F. Diederich, *Angew. Chem. Int. Ed.*, **2003**, *42*, 1486-1490. (*c*) X. Liu, J. Zhou, T. Yu, C. Chen, Q. Cheng, K. Sengupta, Y. Huang, H. Li, C. Liu, Y. Wang, P. Posocco, M. Wang, Q. Cui, S. Giorgio, M. Fermeglia, F. Qu, S. Pricl, Y. Shi, Z. Liang, P. Rocchi, J. J. Rossi, L. Peng, *Angew. Chem. Int. Ed.*, **2014**, *53*, 11822-11827.

[7] (*a*) I. Van der Woude, A. Wagenaar, A. A. P. Meekel, M. B. A. Ter Beest. M. H. J. Ruiters, J. B. F. N. Engberts, D. Hoekstra, *Proc. Natl. Acad. Sci. USA*, **1997**, *94*, 1160-1165. (*b*) H. S. Rosenzweig, V. A. Rakhamanova, R. C. MacDonald, *Bioconjugate Chem.*, **2001**, *12*, 258-263. (*c*) R. Koynova, B. Tenchov, L. Wang, R. C. MacDonald, *Mol. Pharm.*, **2009**, *6*, 951-958. (*d*) M. Dittrich, M. Heinze, C. Wölk, S. S. Funari, B. Dobner, H. Mohwald, G. Brezesinkski, *ChemPhysChem*, **2011**, *12*, 2328-2337. (*e*) W. Zhao, A. A. Gurtovenko, I. Vattulainen, M. Karttunen, *J. Phys. Chem. B*, **2012**, *116*, 269-276.

[8] For reviews see: (*a*) A. Barnard, D. K. Smith, *Angew. Chem. Int. Ed.*, **2012**, *51*, 6572-6581. (*b*) E. Bartolami, C. Bouillon, P. Dumy, S. Ulrich, *Chem. Commun.* **2016**, *52*, 4257-4273. For some key examples see: (*c*) J. E. Kingery-Wood, K. W. Williams, G. B. Sigal, G. M. Whitesides, *J. Am. Chem. Soc.* **1992**, *114*, 7303-7305. (*d*) B. S. Kim, D. J. Hong, J. Bae, M. Lee, *J. Am. Chem. Soc.*, **2005**, *127*, 16333-16337. (*e*) M. K. Müller, L. Brunsveld, *Angew. Chem. Int. Ed.*, **2009**, *48*, 2921-2924. (*f*) E. L. Dane, A. E. Ballok, G. A. O'Toole, M. W. Grinstaff, *Chem. Sci.*, **2014**, *5*, 551-557.

[9] C. Fasting, C. A. Schalley, M. Weber, O. Seitz, S. Hecht, B. Koksch, J. Dernedde, C. Graf, E. W. Knapp, R. Haag, *Angew. Chem. Int. Ed.*, **2012**, *51*, 10472-10498.

[10] (*a*) S. P. Jones, N. P. Gabrielson, D. W. Pack, D. K. Smith, *Chem. Commun.*, **2008**, 4700-4702. (*b*) A. Barnard, P. Posocco, S. Pricl, M. Calderon, R. Haag, M. E. Hwang, V. W. T. Shum, D. W. Pack, D. K. Smith, *J. Am. Chem. Soc.*, **2011**, *133*, 20288-20300. (*c*) A. Tschiche, A. M. Staedtler, S. Malhotra, H. Bauer, C. Böttcher, S. Sharbati, M. Calderon, M. Koch, T. M. Zollner, A. Barnard, D. K. Smith, R. Einspanier, N. Schmidt, R. Haag, *J. Mater. Chem. B*, **2014**, *2*, 2153-2167.

[11] (*a*) K. Rajangam, H. A. Behanna, M. J. Hui, X. Han, J. F. Hulvat, J. W. Lomasney, S. I. Stupp, *Nano Lett.*, **2006**, *6*, 2086-2090. (*b*) A. C. Rodrigo, A. Barnard, J. Cooper, D. K. Smith, *Angew. Chem. Int. Ed.*, **2011**, *50*, 4675-4679. (*c*) S. M. Bromfield, P. Posocco, C. W. Chan, M. Calderon, S. E. Guimond, J. E. Turnbull, S. Pricl, D. K. Smith, *Chem. Sci.*, **2014**, *5*, 1484-1492. (*d*) G. L. Montalvo, Y. Zhang, T. M. Young, M. J. Costanzo, K. B. Freeman, J. Wang, D. J. Clements, E. Magavern, R. W. Kavash, R. W. Scott, D. H. Liu, W. F. DeGrado, *ACS Chem. Biol.*, **2014**, *9*, 967-975. (*e*) T. Noguchi, B. Roy, D. Yoshihara, J. Sakamoto, T. Yamamoto, S. Shinkai, *Angew. Chem. Int. Ed.,* **2016**, *55*, 5708-5712. (*f*) C. W. Chan, D. K. Smith, *Chem. Commun.* **2016**, *52*, 3785-3788.

[12] (*a*) A. Perico, A. Ciferri, *Chem. Eur. J.*, **2009**, *15*, 6312-6320. (*b*) D. Li, N. J. Wagner, *J. Am. Chem. Soc.*, **2013**, *135*, 17547-17555. (*c*) M. S. Sulatha, U. Natarajan, *J. Phys. Chem. B*, **2015**, *119*, 12526-12539.

[13] L. E. Fechner, B. Albanyan, V. M. P. Vieira, E. Laurini, P. Posocco, S. Pricl, D. K. Smith, *Chem. Sci.* **2016**, *7*, 4653-4659.

[14] (*a*) S. M. Bromfield, D. K. Smith, *J. Am. Chem. Soc.*, **2015**, *137*, 10056-10059. (*b*) C. W. Chan, E. Laurini, P. Posocco, S. Pricl, D. K. Smith, *Chem. Commun.* **2016**, *52*, 10540-10543.

[15] For a review see: P. Posocco, E. Laurini, V. Dal Col, D. Marson, K. Karatasos, M. Fermeglia, S. Pricl, *Curr. Med. Chem.*, **2012**, *19*, 5062-5087.

[16] M. C. A. Stuart, J. C. van de Pas, J. B. F. N. Engberts, *J. Phys. Org. Chem.* **2005**, *18*, 929-934

[17] F. D. Gunstone, *Fatty Acid and Lipid Chemistry*, Springer, **1996**.

[18] (*a*) S. M. Bromfield, A. Barnard, P. Posocco, M. Fermeglia, S. Pricl, D. K. Smith, *J. Am. Chem. Soc.*, **2013**, *135*, 2911-2914. (*b*) S. M. Bromfield, P. Posocco, M. Fermeglia, S. Pricl, J. Rodríguez-López, D. K. Smith, *Chem. Commun.*, **2013**, *49*, 4830-4832.

[19] (*a*) B. F. Cain, B. C. Baguley, W. A. Denny, *J. Med. Chem.*, **1978**, *21*, 658-668. (*b*) D. L. Boger, B. E. Fink, S. R. Brunette, W. C. Tse, M. P. Hedrick, *J. Am. Chem. Soc.*, **2001**, *123*, 5878-5891

[20] (*a*) A. J. Konop, R. H. Colby, *Langmuir*, **1999**, *15*, 58-65. (*b*) H. Schiessel, M. D. Correa-Rodriguez, S. Rudiuk, D. Baigl, K. Yoshikawa, *Soft Matter*, **2012**, *8*, 9406-9411.

[21] V. M. P. Vieira, V. Liljeström, P. Posocco, E. Laurini, S. Pricl, M. A. Kostiainen, D. K. Smith, *J. Mater. Chem. B* **2017**, *5*, 341-347.

[22] (*a*) A. Barnard, P. Posocco, M. Fermeglia, A. Tschiche, M. Calderon, S. Pricl, D. K. Smith, *Org Biomol Chem.* **2014**, *12*, 446-455. (*b*) C. Chen, P. Posocco, X. Liu, Q. Cheng, E. Laurini, J. Zhou, C. Liu, Y. Wang, J. Tang, V. D. Col, T. Yu, S. Giorgio, M. Fermeglia, F. Qu, Z. Liang, J. J. Rossi, M. Liu, P. Rocchi, S. Pricl, L. Peng, *Small*, **2016**, *12*, 3667-3676

[23] S. M. Bromfield, P. Posocco, M. Fermeglia, J. Tolosa, A. Herreros-López, S. Pricl, J. Rodriguez-López, D. K. Smith, *Chem. Eur. J.*, **2014**, *20*, 9666-9674.

10.1002/chem.201700177

WILEY-VCH

Entry for the Table of Contents

FULL PAPER

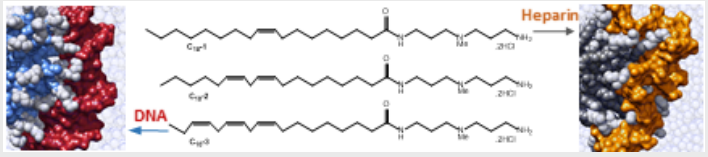

The inside controls the outside. Structural changes to the hydrophobic units direct self-assembly and control the display of cationic ligands on the surface of SAMul nanostructures – DNA and heparin then show different binding preferences to the surface ligands.

*Buthaina Albanyan, Erik Laurini, Paola Posocco, Sabrina Pricl, and David K Smith**

Page No. – Page No.

Self-Assembled Multivalent (SAMul) Polyanion Binding – Impact of Hydrophobic Modifications in the Micellar Core on DNA and Heparin Binding at the Peripheral Cationic Ligands